CHAPTER 94

ROLLER CONTRIBUTIONS AS INFERRED FROM INVERSE MODELLING TECHNIQUES

[1]D.J.R. Walstra, G.P. Mocke, F. Smit
Environmentek, CSIR, PO Box 320, Stellenbosch 7600, South Africa

ABSTRACT
Two independent approaches are discussed whereby inverse modelling is employed as a means of better quantifying roller contributions in the near shore. A so-called integral approach utilizes a coupling between the extended wave energy and momentum balance equations to make inferences regarding roller properties based on wave height and set up measurements. In a somewhat more indirect inverse modelling approach, as first discussed in Mocke et al. (1994), the roller properties are obtained from predicted vertical distributions of internal flow properties such as turbulent kinetic energy, suspended sediment concentrations and undertow velocities which are optimally fitted against measured profiles. An intercomparison between the two approaches is made to get an indication of the validity of the applied theories and inverse modelling techniques. The integral approach further serves to evaluate a new conceptual model for dissipation due to wave breaking

1. INTRODUCTION

Nearshore circulation modelling in wave-dominated environments requires accurate quantification of both wave height and mean water levels across the surf zone. Although attempts at modelling wave height have been relatively successful (Battjes and Janssen, 1978) little progress has been achieved in arriving at a reliable prediction of mean water levels across the surf zone. This is particularly the case for the so-called transition zone immediately following breaking, an area characterized by significant wave height decay whereas the water level remains more or less constant. The observation (Nadaoka and Kondoh, 1982) that the seawards directed return flow or undertow, the primary mechanism for cross-shore sediment transport, attains maximum strength some distance landwards of the breakpoint reinforces the necessity to better quantify this lag effect.

---

[1] Present address: Delft Hydraulics, P O Box 177, 2600 MH Delft, The Netherlands.

Svendsen(1984) incorporated additional contributions of mass and momentum to account for the presence of the aerated water body or "roller" at the water surface in the surf zone. It was however only with later models such as those of Roelvink and Stive(1989) and Nairn et al(1990) that attempts were made to model the extent of the transition zone and the spatial evolution of the roller. These models incorporated a lag between the production and dissipation of turbulent kinetic energy (TKE) arising from the breaking process. More recently, Dally and Brown(1995) propose an empirical roller model wherein the transition zone arises from the interval in time required for roller creation.

2. INVERSE MODELLING APPROACHES

2.1 System of Equations

Integral Properties

The wave energy balance according to Battjes and Janssen (1978) is used to describe the wave height distribution across the surf zone. Only waves travelling perpendicular towards the coast are considered. The wave energy balance is written as:

$$\frac{\partial F_x}{\partial x} = -D_w \qquad (1)$$

Where F_x is the onshore energy flux per unit width and D_w is the time averaged energy dissipation in a breaking wave (LeMehaute, 1962).

With the assumption that breaking waves are modelled as bores travelling towards the coast with the wave celerity (c). Nairn et al. (1990) propose the following equation:

$$\frac{\partial E_w c_g}{\partial x} + \frac{\partial E_R c}{\partial x} + \tau_s c = 0 \qquad (2)$$

where E_R denotes the kinetic energy of the roller and τ_s is the shearstress in the nearsurface. The result given in Deigaard and Fredsoe (1989) that the dissipation originates from the work done by the shear stress due to the roller acting on the fluid right below it is included in the third term of Equation 2 (i.e. $D_R = \tau_s c$).

The properties of the roller are described according to Svendsen (1984):

$$E_R = \frac{\frac{1}{2} m_r c^2}{L} = \rho A \frac{c^2}{2L} = \frac{\rho A c}{2T} \qquad (3)$$

For the derivation of the dissipation in the roller, D_R, the findings of Deigaard and Fredsoe (1989) are used again to relate the shear stress exerted by the roller onto the underlying wave to this dissipation. The shear stress is derived under the assumption that the position of the roller does not change relative to the underlying wave. This implies that the shear stress induced by the roller should balance the downward force exerted on the roller due to gravity. D_R is then written as:

$$D_R = \tau_s c = \beta\rho g \frac{A}{L} c = \beta\rho g \frac{A}{T} \quad (4)$$

In which A is the cross-sectional area of the roller, T is the wave period, β is the slope of the wave front, and L is the wave length.

Incorporating a contribution due to the wave roller the time averaged momentum equation reads:

$$\left(2\frac{c_g}{c} - \frac{1}{2} \right) \frac{\partial E_w}{\partial x} + M_r + \rho g h \frac{\partial \eta}{\partial x} = 0 \quad (5)$$

De Vriend and Kitou (1990) presented an analysis in which for the case of spatially varying waves on a sloping bottom the orbital velocity moments were derived. Based on these results Stive and De Vriend (1994) derived an expression for the vertical shear stress distribution in case of a sloping bottom and wave breaking dissipation. At the water surface this expression reads:

$$\tau_t = -\frac{1}{c} \frac{\partial E_w c_g}{\partial x} - M_R \quad (6)$$

The second term on the right-hand side has to be interpreted as the time averaged gradient of momentum in the roller. Using the roller concept (Equations 3 and 4) M_R can be written in terms of the kinetic energy of the roller which yields:

$$M_R = 2\frac{\partial E_R}{\partial x} \quad (7)$$

By inserting Equation 7 into Equation 6 the energy balance obtained from the momentum balance results:

$$\frac{\partial E_w c_g}{\partial x} + 2\frac{\partial E_R c}{\partial x} + \tau_s c = 0 \quad (8)$$

The wave celerity c has been included in the gradient of the energy flux of the roller, which is acceptable if it is assumed that the spatial variations in wave celerity are small relative to those in E_R.

Comparing Equations 8 and 2 an apparent inconsistency is visible; there is a factor 2 difference in the term in which E_R appears. This inconsistency was clarified by Deigaard (1993), as discussed in Stive and De Vriend (1994). Deigaard (1993) found that the inconsistency arises from the complicated situation that occurs when the volume of the roller is changing in the wave propagation direction. Besides the shear layer between the roller and the wave there is a net transfer of water from the wave to the roller as the volume of the roller increases, and vice versa if the volume of the roller decreases. This implies that an additional momentum exchange between the roller and the underlying wave is present. The corrections that these considerations give to the shear stress and to the energy balance remove the inconsistency resulting

in an energy balance with the factor 2 included.

Flow Properties

According to 2DV momentum balance considerations, equilibrium between the depth-integrated wave induced momentum flux (i.e. the radiation stress and the set-up gradient) yields a depth-mean zero flow. However, due to the fact that mass and momentum fluxes need not be in balance at any point through the depth a secondary return flow known as the undertow may result.

The undertow equation, which follows from a combination of the local and horizontal momentum balances, has the form (assuming a wave-averaged eddy viscosity for approximation of the Reynolds stresses):

$$\frac{\partial}{\partial z}\left(\nu_t \frac{\partial U}{\partial z}\right) = \frac{\partial}{\partial x}\left(\overline{u^2} - \overline{w^2}\right) + \frac{\partial}{\partial x} g\overline{\eta_x} + \frac{\partial}{\partial z}\left(\overline{uw}\right) \qquad (11)$$

where U is the wave-averaged return flow or undertow, η_x is the mean watcr level set-up, and u and w are the horizontal and vertical wave-orbital velocities.

For the considered wave-averaged situation the above equation is presumed to be valid from the bottom boundary to the vicinity of the surface.

As discussed by Stive and De Vriend (1994), wave averaged shear stresses are solely due to wave amplitude variations associated with shoaling, and dissipation due to boundary layer shear and/or breaking waves. From a quantification of the wave-related terms, the depth variation of eddy viscosity, the mean mass flux above wave trough level and the shear stress at mean water level may be resolved the undertow variation over depth.

The roller effects of the near surface layer (NSL) are manifested through a shear stress τ_s acting at the mean water level. Hence the upper boundary condition corresponds to:

$$\nu_t \frac{\partial U}{\partial z} = \frac{\tau_s}{\rho} \quad at \; z = z_s \qquad (12)$$

A no slip condition applies at the bottom boundary:

$$U = 0 \quad at \; z = 0 \qquad (13)$$

According to mass balance considerations the total mass flux (M) in the lower layers balances that in the NSL, from which can be derived the set-up gradient. The assumption is made that the wave terms (orbital velocity movements) can be derived independently from the mean flow. Based on a derivation by Bijker (1974), Stive and De Vriend (1994) proposed approximations for the time-averaged values of the wave terms defined in Equation 11. These are incorporated in the present model. For the determination of the depth dependant eddy viscosity (ν_t) use is made of a two

equation (k-ε) turbulence model wherein the dissipation due to wave breaking is the primary forcing term (Mocke and Smith, 1992).

The time-mean vertical distribution of suspended sediment is described by the classical equation describing a balance between an upward flux due to eddy-diffusion and a downward settling component:

$$0 = D_c \frac{\partial C}{\partial z} + w_s C \qquad (14)$$

where C is the suspended sediment concentration, w_s the sediment fall velocity and D_c the sediment diffusion or mixing coefficient. The diffusion coefficient is generally assumed proportional to the eddy viscosity.

2.2 Inverse Modelling Procedures

Integral Properties

The inverse modelling procedure using integral properties is illustrated in the flow chart shown in Figure 1. The initial step entails use of the extended momentum equation (Equation 6). Since the wave height and set up are known from measurements the term M_R can be determined directly (inverse model results have a subscript "*inv*", and the measured results are extended with the subscript "*meas*"):

$$M_{R_{inv}} = -\rho g \left(\left(\frac{1}{4}\frac{c_g}{c} - \frac{1}{16} \right) \frac{\partial H^2_{meas}}{\partial x} + h_{meas} \frac{\partial \eta_{meas}}{\partial x} \right) \qquad \textbf{(13)}$$

Integrating Equation 8 results in the kinetic energy present in the roller:

$$E_{R_{inv}}(x) = \frac{1}{2} \int_{x=x_b}^{x} M_{R_{inv}} dx + E_{R_{inv}}(x=x_b) \qquad \textbf{(14)}$$

in which the second term on the right hand-side is zero by definition.

The dissipation in the roller, D_R, can be calculated from the energy balance in which the term M_{Rinv} obtained from the momentum equation is used to determine the gradient of the energy flux in the roller:

$$D_{R_{inv}} = -\frac{1}{8}\rho g \frac{\partial \left(H^2_{meas} c_g \right)}{\partial x} - c M_{R_{inv}} \qquad \textbf{(15)}$$

Note the fact that in the equation above the assumption that the spatial variations of c are small compared to those of E_{Rinv} is used.

With the inverse model it is now possible to determine the dissipation in the roller D_R directly from the momentum equation. The only assumption that has to be made is Equation 7 which gives the connection between the momentum and energy balance. The assumption that the spatial variation of the wave celerity can be neglected

compared to the variation of the energy in the roller is not expected to influence the results dramatically.

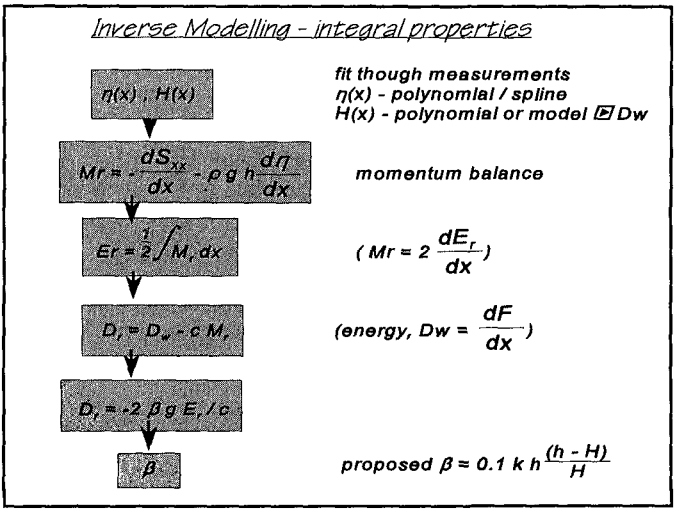

Figure 1 Inverse modelling procedure

Having determined E_r using the momentum equation and D_r using the wave energy balance, an inverse modelled β can be found applying the roller approach according to Svendsen (1984):

$$\beta = \frac{D_r c}{2gE_r} \tag{16}$$

A number of studies have concluded that a constant value of 0.1 gives the best set up results (e.g. Roelvink, 1993).

Following a spline smoothing interpolation of wave height and set up measurements, the procedure outlined above is followed and the cross shore distribution of E_r, D_r, and β are calculated.

Flow Properties

As the most readily available and reliable set of flow measurements, the inverse modelling analysis is carried out principally on undertow data. Limited investigation has however also been carried out using TKE and sediment concentration measurements. The analysis procedure for undertow measurements is illustrated in the flowchart shown in Figure 2. A first estimate of D_r is made using the transition zone model of Nairn et al(1990), however the exercise could also conceivably start with D_w as a first estimate of D_r. With D_r and the wave induced mass flux the independant variables, an optimal combination having least rms error between measured and computed velocities is determined.

The analysis procedures for TKE and concentrations is somewhat simpler in that the sole variable is D_r, the source of TKE production at the surface boundary.

3. RESULTS

Integral Properties

Presented in Figure 3 is a step-by-step illustration of an application of the inverse integral modelling approach. Depicted in Figures 3(a) and (b) are measured wave heights(H) and mean water levels(η) for test 1 of Stive(1983). This case corresponds to a monochromatic spilling type wave (Ho=0.16m , T=1.8s) with breaking induced on a plane 1:40 beach slope. Using a polynomial fitting procedure a continuous representation of the cross-shore distribution of wave heights and mean water levels is obtained.

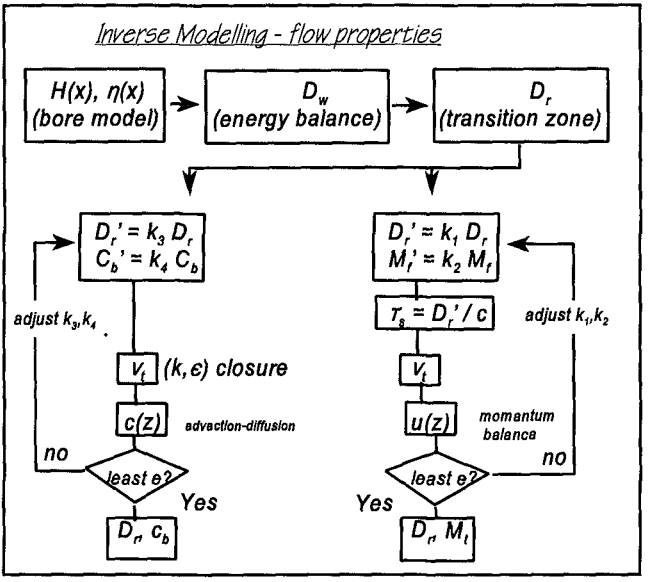

Figure 2 Analysis procedure for undertow measurements

The corresponding cross-shore distribution of wave energy dissipation(D_w), calculated from Equation 1 using linear, 2nd order cnoidal and covocoidal theory, is shown in Figure 3(c).These distributions demonstrate a prominent peak in D_w immediately following the break point, reflecting the observed rapid attenuation in wave height after breaking.

The fitted wave heights are subsequently used to compute the radiation stress distribution. As illustrated in Figure 3(d) these estimates are highly dependant on the wave theory employed. Also plotted in this figure are measurements of radiation stress made by Stive (1983). The generally accepted tendency for linear theory to significantly overestimate radiation stress in the vicinity of the breaking point is clearly demonstrated. It may further be remarked that although the covocoidal theory provides improved estimates in this region, linear theory is in close correspondence with radiation stress measurements made in the inner surf zone.

Figure 3(e) presents the results of the following step, whereby the cross-shore radiation stress and mean water level distributions are introduced in Equation 16 to solve for Mrinv. In much the same manner as for D_w, the M_r distribution demonstrates a prominent peak immediately post-breaking. This is consistent with a transfer of momentum to this roller storage term through the initial transition zone. M_r

subsequently attains negative magnitudes in the inner surf zone where excess momentum is transferred from the roller into the underlying flow.

The roller energy E_r distribution is obtained from M_r using Equation 17. As depicted in Figure 3(f) this parameter has a peak significantly shorewards of the breaking point. This feature is consistent with physical reality, whereby the wave roller is only fully established at the limit of the transition zone.

Using Equation 18 the wave roller dissipation can subsequently be obtained from energy balance. As illustrated in Figure 3(g) this parameter shows a landwards shift in peak value as had been observed for Er. The Dr distribution can further be seen to be very much different from that previously found for Dw.

From Equation 19 relating D_r to the roller geometry and E_r the cross-shore distribution of the roller slope may be resolved. For the case under consideration it may be seen from Figure 3(h) that a constant value of the order 0.1 as proposed by Nairn et

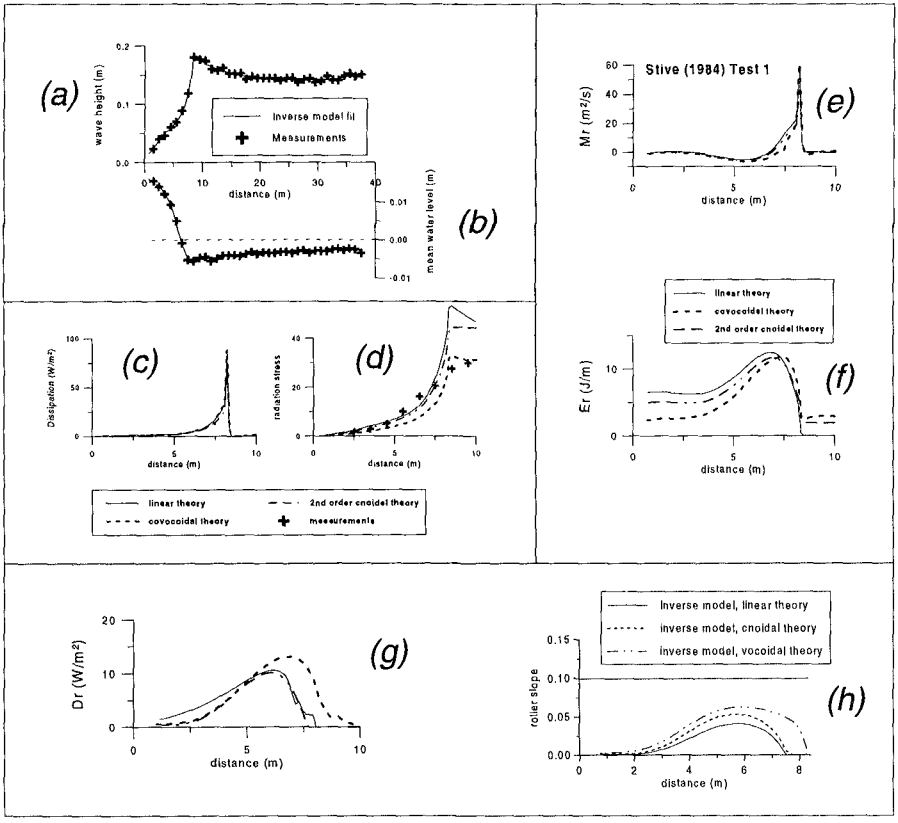

Figure 3 Step-by-step illustration of an application of the inverse integral modelling approach

al(1990) is inappropriate.

For the case of random waves principal reference is made to the LIP11D measurements made in the large scale Delta Flume. For a description of these tests reference should be made to Arcilla et al(1993).

In Figure 4 is shown the fitted H_{rms} and η distributions for measurements made mid-way through test 1A. For the H_{rms} measurements a Battjes and Janssen(1978) type bore model is run until an optimal fit is obtained whilst a spline curve is used for the water level. Using a similar procedure to that described previously for the monochromatic wave case, Figure 5 shows the constituent terms of the momentum balance equation. An initial increase in M_r, coincident with increased wave breaking, is followed by rapid decrease to negative values as both the radiation stress and set-up term increase. Figure 6 depicts cross-shore distributions of D_w and D_r, under linear and covocoidal wave theories, for the same case. Although the two wave theories result in very different D_w distributions the inverse modelled D_r distributions are in reasonably good accordance. Although linear theory does not attain the same peak value at around X=148m both theories show a distinet landwards shift from the Dw distribution.

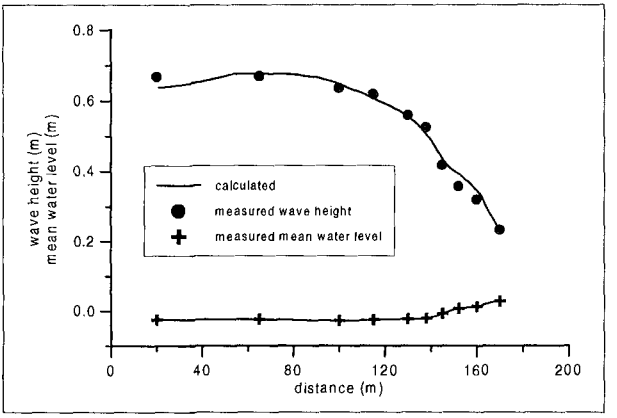

Figure 4 Fitted Hrms and eta distributions for measurements of LIP test 1A.

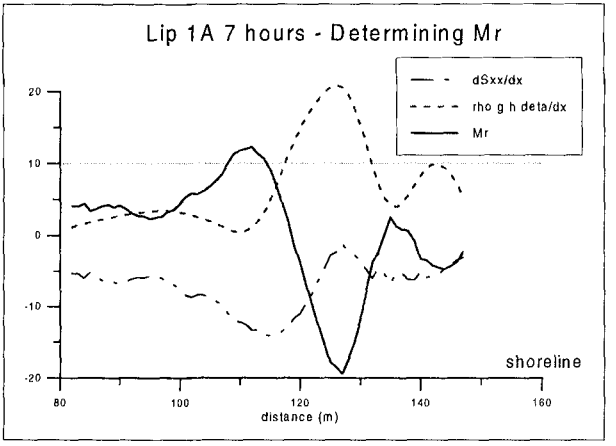

Figure 5 Constituent terms of the momentum balance equation

Model sensitivity

The sensitivity of the inverse modelling procedure to measured mean water levels is illustrated in Figure 7. Depicted in Figure 7(a) are spline fits of the mean water level as recorded on four occassions during Test 1A. Figure 7(b) shows the corresponding Dr distributions for each of the 4 measuring instances. Although water levels do not change by more than about 1cm there are distinct differences between the modelled D_r dsitributions. This is particularly the case for the situation after 7 hours where a dip in the water level near X=120m results in a D_r peak not evident for other times. On the whole however the principal features of the cross-shore distribution of D_r appear to be consistent.

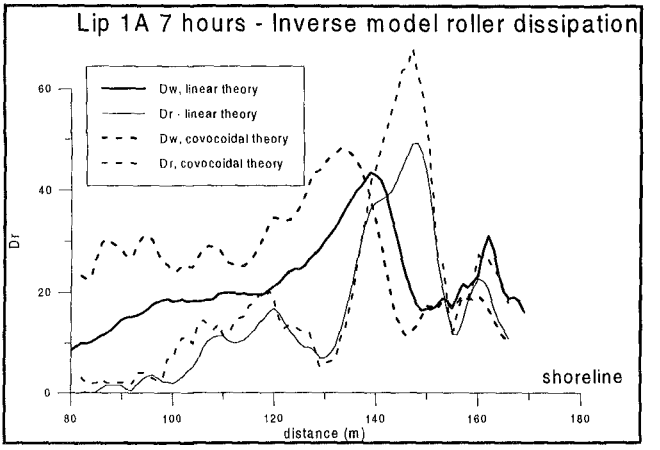

Figure 6 Cross-shore distributions of Dw and Dr, under linear and covocoidal wave theories for Lip Test 1A

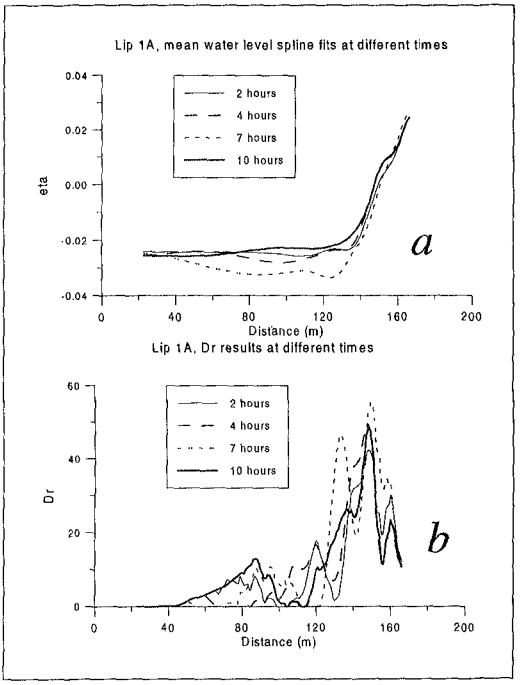

Figure 7 Sensitivity of the inverse modelling procedure to measured mean water levels

Slope of wavefront

A principle finding is that β is not constant for all the investigated theories. A new β will be defined which is derived for linear wave theory. The old definition of β being the slope of the wave front is extended with an additional factor that takes the internal dissipation of roller energy into account. Attention is primarily focussed on predicting β in the area where the external roller dissipation is non-zero or relatively large for respectively mono-chromatic and random waves.

An extensive statistical analysis of waveflume experiments (Stive, 1983, Buhr Hansen and Svendsen, 1984, Arcilla et al, 1993) resulted in the following expression for β:

$$\beta = 0.1kh\frac{h - H}{H} \quad \wedge \quad <0.1 \tag{17}$$

in which k is the wave number, H is the wave height, and h is the water depth.

In Figure 8a the inverse β and the approximation given by Equation 20 are compared for the Stive tests. It is clear from all tests that the proposed simple expression does give a surprising good result. Although β should be zero pre-breaking it also shown for that region so as to indicate the performance of the suggested expression. Even the location at which the dissipation of kinetic energy is initiated is well approximated for most of the tests as the minimum value of the proposed expression for β gives a reasonably accurate indication of this position. Figure 8b the performance of the proposed expression for beta is shown for a number of sets from LIP11D test 2B. Although the variation of the inverse modelled beta are considerable a distinct trend is visible which is represented reasonably by the proposed expression for beta.

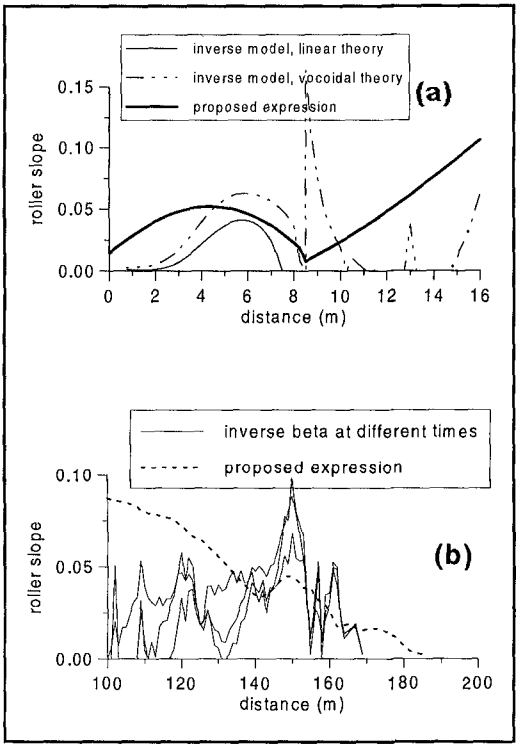

Figure 8 Inverse roller slope and slope expression for (a) Stive test 1 and (b) LIP 1A

Flow Properties

The predicted vertical distributions of TKE shown in Figure 8 are obtained by adjusting Dr so as to minimize the rms error between measurements and predictions. Although the model tends to demonstrate slightly more vertical variability than the measurements of Stive(1983) it is likely that the measurements in the upper part of the water column have been contaminated somewhat due to aeration associated with the breaking process.

Figure 9 depicts the optimal undertow fit for the same test case of Stive(1983). In this inverse modelling procedure both Dr and the wave induced mass flux contribution are adjusted independantly until the rms error is minimized. The precision of this exercise is limited however by the existence of measurements over only part of the depth.

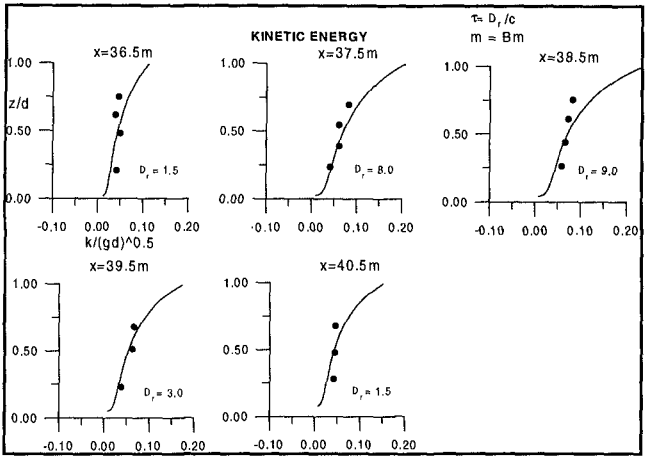

Figure 9 Predicted vertical distributions of TKE for Stive Case 1

As can be seen in Figure 10 the optimal correspondance between measurements and predictions for the LIP11D cases was in most cases very good, with rms errors generally less than 5%.

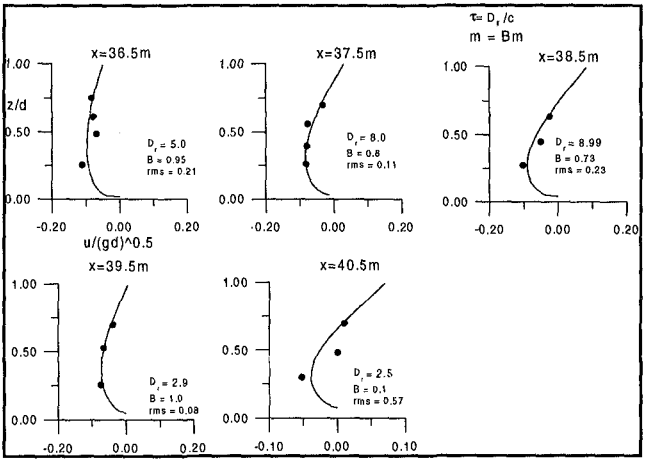

Figure 10 Optimal undertow fit for the Stive case 1

Intercomparisons

The inverse modelled Dr distributions using the integral approach have been found to differ markedly from those for Dw. Figure 11 compares estimates of Dr as determined by the integral approach and the inverse fits of TKE and undertow measurements for Stive Test 1.

Both inverse approaches show a similar cross-shore distribution and suggest a peak in Dr some 3m landwards of the break point. As previously observed this lag has important implications for localizing the point of maxima for cross-shore and longshore currents and sediment suspension and transport.

Figure 12 compares Dw and inverse modelled Dr distributions for LIP(t=7hrs) case 1A. In general the independant inverse modelling approaches are in good correspondance, with a noticeable landwards shift in the position of Dr peaks relative to Dw. For the cases under consideration such shifts are far from negligible, generally exceeding 10m. Also plotted in Figure 12 are the predicted Dr distributions using both a constant and variable beta value. Although these distributions are in generally close accord to that found by inverse modelling, the lag effect is somewhat underestimated.

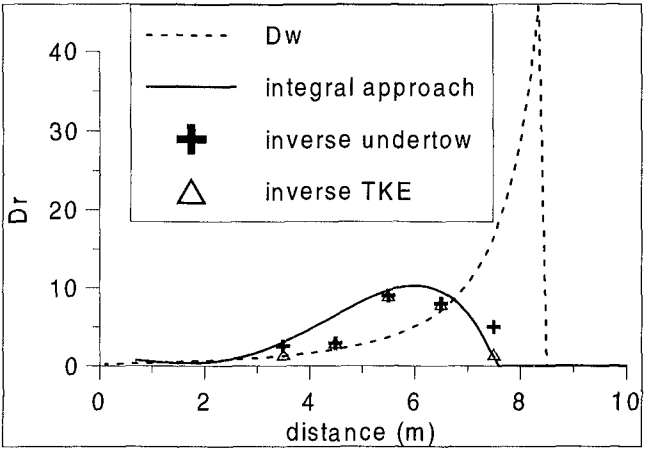

Figure 12 Estimates of Dr for Stive Test 1

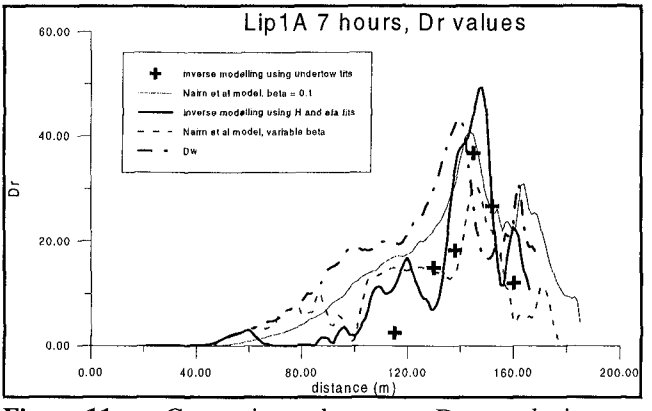

Figure 11 Comparison between Dw and inverse modelled Dr distributions for LIP(t=7hrs) case 1A

4. CONCLUSIONS

Due to the good agreement between both inverse modelling techniques a strong indication of the validity of both approaches and applied theories is obtained. The two independant inverse modelling techniques clearly indicate a landward shift of the maximum roller energy dissipation compared to the wave dissipation. This suggests that the apparent landwards shift for maxima of TKE, undertow and suspended sediment concentrations and consequently cross-shore and longshore sediment transport rates can only be obtained by accurately predicting the cross-shore distribution of wave heights and especially the mean waterlevel. Although the integral appoach is sensitive to the accuracy of wave and water level measurements it can provide continous cross-shore distributions of roller properties. Recent experiments

provide additional types of data such as the measurement of the roller slope (e.g. Boers, 1996) which can be used to verify the roller expressions proposed by Svendsen (e.g. area of the roller and slope of wave front) and improve the proposed expression for beta.

REFERENCES

Arcilla, A.S., Roelvink, J.A.,O'connor, B.A., Reniers, A., Jiménez, J.A., 1994. The Delta flume'93 Experiment. *Proc. Coastal Dynamics Conf.*

Battjes, J.A., Janssen, J.P.F.M.,1978. Energy loss and Setup due to breaking of random waves. *Proc. 16th Coastal Eng. Conf.*

Bijker, E.W. 1974. Mass transport of gravity waves on a sloping bottom. *Proc. 14th Coastal Eng. Conf.*

Boers, M., 1996. Simulation of a Surfzone with a Barred Beach. Report 1: Wave Heights and Wave Breaking. *Communications on Hydraulic and Geotechnical Engineering Report no 96-5,* Delft University of Technology.

Buhr Hansen, J. and Svendsen, I.A., 1984. A theoretical and experimental study of undertow. *Proc. 19th Coastal Eng. Conf.*

Dally,W.R. and Brown, C.A., 1995. A modelling investigation of the breaking wave roller with application to cross-shore currents. *J Geophys Res.*, 100, C12.

Deigaard, R., 1993. A note on the three-dimensional shear stress distribution in a surf zone. *Coastal Eng.,* **20**, 157-171.

Deigaard, R. and Fredsoe, J., 1989. Shear stress distribution in dissipative water waves. *Coastal Eng.*, **13**, 357-378.

De Vriend, H.J. and Kitou, N., 1990. Incorporation of wave effects in a 3D hydrostatic mean current model, *Proc. 22nd Coastal Eng. Conf.*

Le Mehauté, B., 1962. On non-saturated breakers and the wave run-up. *Proc. 8th Coastal Eng. Conf.*

Mocke, G.P., Reniers, A., Smith, G.G., 1994. A surf zone parameter sensitivity analysis on LIP11D suspended sediment and return flow measurements. *Proc. Coastal Dynamics Conf.*

Mocke, G.P., Smith, G.G., 1992. Wave breaker turbulence as a mechanism for sediment suspension, *Proc. 23rd Coastal Eng. Conf.*

Nadaoko, K. and Kondoh, T. (1982). Laboratory Measurements of Velocity Field Structure in the Surf Zone by LDV. *Coastal Engineering in Japan*, **25**, 125-145.

Nairn, R.B., Roelvink, J.A., Southgate, H.N., 1990. Transition zone width and implications for modelling surf zone dynamics. *Proc 22nd Coastal Eng. Conf.*

Okayasu, A., 1989. Characteristics of turbulence structure and undertow in the surf zone. *Ph.D. thesis*, Yokohama Nat. Univ.

Roelvink, J.A., 1993. Surface roller effect in a surfbeat model. *G8 Coastal Morphodynamics*, Grenoble Overall Workshop.

Stive, M.J.F., De Vriend, H.J., 1994. Shear stresses and mean flow in shoaling and breaking waves. *Proc. 24th Coastal Eng. Conf.*

Stive, M.J.F., 1983. Two dimensional breaking of waves on a beach. *Delft Hydraulics report M1585.*

Svendsen, I.A. 1984. Mass flux and undertow in the surf zone. *Coastal Eng.*, 8(4).